THE ASTROPHYSICAL JOURNAL, 351:364–376, 1990 March 10

THE LYMAN LIMIT ABSORPTION SYSTEM IN THE SPECTRUM OF PKS 2126−158: HEAVY-ELEMENT ABUNDANCE AT HIGH REDSHIFT

WALLACE L. W. SARGENT AND CHARLES C. STEIDEL
Palomar Observatory, California Institute of Technology

AND

A. BOKSENBERG
Royal Greenwich Observatory
Received 1989 May 24; accepted 1989 September 9

ABSTRACT

We have investigated the heavy element composition of a Lyman limit absorption system at $z_{abs} = 2.9676$ in the spectrum of PKS 2126−158 ($z_{em} = 3.27$). Early observations had suggested that this absorption system had no detectable lines of heavy elements; however, the observations reported here reveal weak associated lines due to C IV and C II. We have used photoionization models to show that the system has [C/H] = -2.3 ± 0.2 and [Si/H] ≤ -2.3. We discuss the possibility that the $z_{abs} = 2.9676$ system in PKS 2126−158 is produced in galactic halo material or by primitive gas-rich dwarf galaxies.

Subject headings: abundances — cosmology — galaxies: structure — quasars

I. INTRODUCTION

PKS 2126−158 was identified as a QSO with an emission redshift $z_{em} = 3.27$ by Jauncey *et al.* (1978). At magnitude 17.3 it is one of the brightest QSOs of very high redshift. Consequently, PKS 2126−158 was the first QSO with $z_{em} \geq 3$ to be studied at high (0.8 Å) spectral resolution (Young *et al.* 1979). These observations were made at the Anglo-Australian Telescope and covered the wavelength range $\lambda\lambda$4153–6807, although the signal-to-noise ratios of the data were not high by present-day standards. The detailed analysis by Young *et al.* revealed the existence of two certain absorption systems, at $z_{abs} = 2.6381$ and $z_{abs} = 2.7685$ were identified, together with a less certain system at $z_{abs} = 2.3938$. At the 1983 Liège Symposium, Sargent and Boksenberg (1983) reported the discovery of a Lyman limit absorption system at $z_{abs} = 2.9682$[1] in the spectrum of PKS 2126−158. This system produces a Lyman edge at λ3643, thus falling shortward of the spectral range covered by the earlier AAT observations. The Palomar IPCS spectra in which the Lyman limit was found will be described in the present paper. Sargent and Boksenberg reported finding several lines of the Lyman series associated with the Lyman limit system, but no certain lines of heavier elements. The H I column density was well determined to be log N(H I) = 17.3, with a velocity dispersion $\sigma_v = 23 \pm 1$ km s^{-1}. Possible lines of the O VI $\lambda\lambda$1031, 1037 doublet were found. However, the λ1307 line was observed to be stronger than λ1031; moreover, the feature identified as λ1031 was blended with a strong line supposed to be a Lyman-α absorption line. The estimated upper limit to the O VI column density was N(O VI) $\leq 2 \times 10^{14}$ cm^{-2}, thus giving rise to an upper limit for the O VI to H I abundance ratio of [log (O VI/H I)] ≤ -2.9. This result was of interest because Norris, Hartwick, and Peterson (1983) had used a statistical method to search for weak heavy element lines associated with the lines of the Lyman-α forest and had claimed to detect the O VI doublet in Q0805−046 ($z_{em} = 2.88$) and Q1442+101 (OQ 172; $z_{em} = 3.53$) with 99% confidence. The corresponding O VI to H I ratio was log (O VI/H I) ≤ -1.1, in clear conflict with Sargent and Boksenberg's result quoted above.

Meyer and York (1987) obtained spectra of PKS 2126−158 over a limited wavelength range with very high S/N, but moderate (~2 Å) resolution. They identified several previously undetected weak C IV doublets, and concluded that many of the strong Lyman-α lines in the Lyman-α forest have detectable heavy element lines at the same redshift. However, Meyer and York explicitly did not rule out the possibility that "the vast majority of Lyman-α systems are metal-free."

In their survey of C IV absorption in the spectra of 55 QSOs, Sargent, Boksenberg, and Steidel (1988, hereinafter SBS) confirmed the redshifts suggested by the earlier work of Young *et al.* (1979) and also several of the systems found by Meyer and York (1987).

Later, in a survey for Lyman limit absorption in a sample of 59 QSOs, Sargent, Steidel, and Boksenberg (1989) obtained a low (~6 Å) resolution spectrum of PKS 2126−158 having very high S/N. Two Lyman limit systems were identified (and in fact, the earlier spectra described by Sargent and Boksenberg 1983 had shown residual flux below the wavelength of the identified Lyman limit). One had $z_{LLS} = 2.792$ and was conjectured to be associated with the already known heavy element absorption system at $z_{abs} = 2.7685$. The Lyman limit system at $z_{LLS} = 2.973$ was observed to have a possible corresponding C IV doublet at $z_{abs} = 2.965$ which, however, was not resolved. This discovery prompted us to undertake new, higher resolution observations of the appropriate spectral regions of PKS 2126−158 in order to estimate the heavy element abundance of what had appeared to have been a candidate for a Lyman limit system arising in a primordial cloud.

II. OBSERVATIONS AND REDUCTIONS

As indicated in § I, spectra of PKS 2126−158 have been obtained with the IPCS detector on both the Anglo-Australian Telescope and with the Double Spectrograph at the Hale Telescope over a number of years. More recently, spectra of very high S/N were obtained with the CCD detectors on the Double Spectrograph. The CCDs have much higher quantum effi-

[1] Due to a typographical error the redshift of the Lyman limit is incorrectly given as $z_{abs} = 2.9982$ in the published paper.

TABLE 1

OBSERVATIONS OF PKS 2126−158

Telescope	Date	Exposure (s)	λ Range (Å)	FWHM (Å)	Reference
AAT.....	1976 Nov	5400	4750–5520	0.87	1
	1976 Nov	6000	4150–4950	0.72	1
	1977 Jun	10000	5150–6260	1.05	1
	1977 Jun	5500	5700–6810	1.05	1
PAL.....	1981 Jun	9000	3760–4415	1.37	2
	1981 Jul	8000	3125–4175	2.65	2
	1984 Oct	7000	4760–6000	1.50	3
	1984 Oct	4000	5800–6950	1.50	3
	1987 Oct	1500	3150–7000	5.00	4
	1988 Oct	7200	4570–5016	1.10	2
	1988 Oct	7200	5901–6556	1.50	2

REFERENCES.—(1) Young *et al.* 1979; (2) this work; (3) Sargent, Boksenberg, and Steidel 1988; (4) Sargent, Steidel, and Boksenberg 1989.

ciency than the IPCS, but cover only about one-third of the wavelength range. However, now that techniques for improving the blue sensitivity of CCDs have been developed, the effective advantage of the IPCS has been lost for many applications in which the CCD readout noise (typically ~10 electrons per pixel for the devices on the Double Spectrograph) is not important. The various observations of PKS 2126−158 are summarized in Table 1. Many of the observations have already been published. Details of the methods of observation and the reductions of the raw data are contained in the references cited in the footnotes to Table 1. Information on the remaining observations will now be given.

a) IPCS Data

The spectrum of the Lyman-α forest region of PKS 2126−158 was observed with the University College London Image Photon Counting System (IPCS) detector installed on the blue camera of the Double Spectrograph at the Cassegrain focus of the Hale 5 m telescope. Two different resolutions were used. On 1981 June 27/28 exposures totaling 9000 s were made at the wavelength region λλ3760–4415. A 1200 groove mm^{-1} grating blazed at λ5000 in the second order was used to give a dispersion of 18 Å mm^{-1}. A liquid copper sulphate filter was used to exclude the first-order red spectrum. The IPCS was used in a mode which gives 1750 pixels along the direction of the dispersion. PKS 2126−158 was low in the sky and the seeing was mediocre—of order 2″. Accordingly, a 2″ × 1′ entrance slit was used; the resulting resolution as judged from measurements of the comparison arc lines was 1.4 Å (FWHM). Observations were made of the spectrophotometric standard star EG 145 in order to establish the relative flux scale.

On the night of 1981 July 3/4, PKS 2126−158 was observed again, this time with a 1200 groove mm^{-1} grating blazed at λ5000 in first order. The dispersion was 36 Å mm^{-1} and a 2.″0 slit was used since the seeing was again only moderately good. The resulting spectrum, obtained with an exposure of 8000 s covered the wavelength range λλ3125–4175 at a resolution of ~2.6 Å(FWHM) and includes the Lyman limit. The standard star EG 145 was again observed for flux calibration. In all the observations the QSO was stationed on four different places along the slit, separated by a few arcseconds, for periods of 1000 seconds. Arc exposures were made each time the QSO was moved to a new position. This procedure has been found to improve the sky subtraction: it also allows small slight wavelength drifts due to flexure in the spectrograph to be compensated.

The reductions were performed in the usual way using the flat fields and standard star observations to calibrate the small- and large-scale pixel-to-pixel responses, respectively. Wavelength scales were established by fitting polynomials to the arc lines; the typical residuals in the wavelength scales were $\sigma = 0.06$ Å for the high-resolution observations and $\sigma = 0.12$ Å for the low-resolution data, respectively.

Plots of the resulting spectra are shown in Figures 1 and 2.

b) CCD Data

Spectra covering the wavelength ranges λλ4570–5016 and λλ5901–6556 were obtained on the night of 1988 October 17 using the Double Spectrograph on the Hale Telescope. The

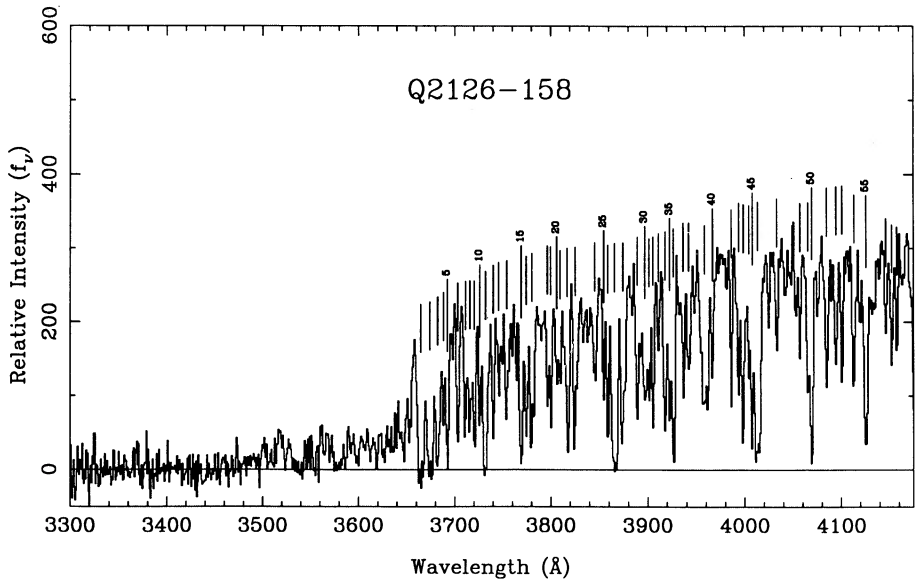

FIG. 1.—IPCS spectrum showing the Lyman discontinuity due to the absorption system at $z_{abs} = 2.9676$. Note the residual flux present below the Lyman limit at ~3620 Å.

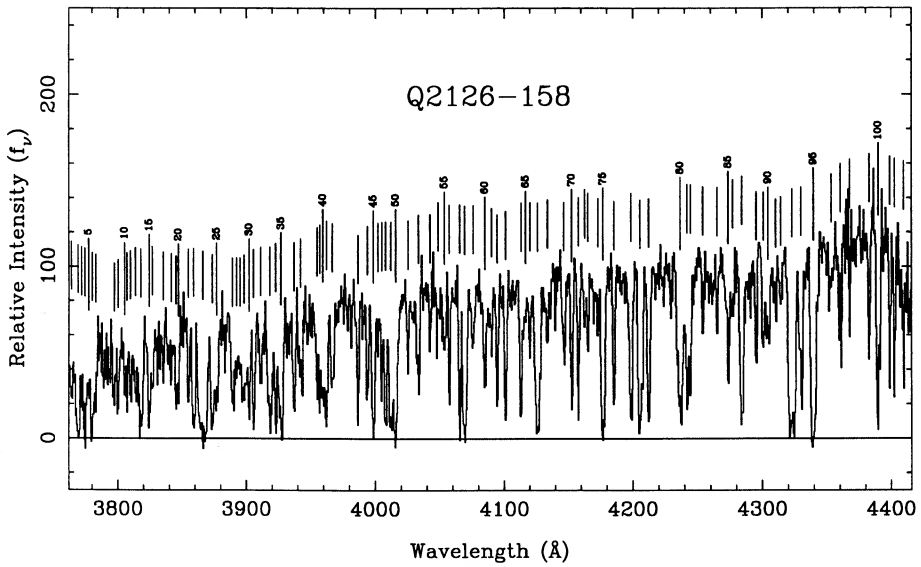

FIG. 2.—IPCS spectrum of PKS 2126−158, with 1.4 Å resolution

two chosen wavelength regions include, respectively, the Lyman-α absorption line at $z_{abs} = 2.97$ and the region expected to contain the corresponding C IV λλ1548, 1550 doublet. The detailed setup and observing procedures were similar to those described by Sargent, Steidel, and Boksenberg (1989), except that 1200 lines mm^{-1} gratings were used in both cameras. The resulting resolution and the exposure times (each broken into two separate exposures of 3600 s to limit the cosmic-ray exposure) are given in Table 1.

Figures 3 and 4 show plots of the resulting spectra.

c) *Absorption Lines*

The absorption lines in the spectra presented in Figures 1, 2, 3, and 4 were measured using the methods outlined by Young *et al.* (1979). All lines which satisfied the criterion $W > 5\,\sigma(W)$ are given in Tables 2–5, and the line positions are indicated in Figures 1–4, respectively. As is well known, the definition of the continuum in the Lyman-α forest region is to some extent subjective, as is the separation of blended lines into individual components. For this reason, the tabulated equivalent widths and wavelengths of lines falling shortward of the Lyman-α emission line are considerably more uncertain than the formal errors would suggest.

III. ABSORPTION REDSHIFTS

Young *et al.* (1979) found only two certain redshift systems, $z_{abs} = 2.6381$ and 2.7685, respectively. One additional system, $z_{abs} = 2.3938$, was regarded as less certain. As part of a survey of C IV absorption as a function of redshift in QSOs (SBS), spectra extending from the C IV emission line down to just below the Lyman-α emission line were searched for heavy-element redshift systems. The three systems identified by

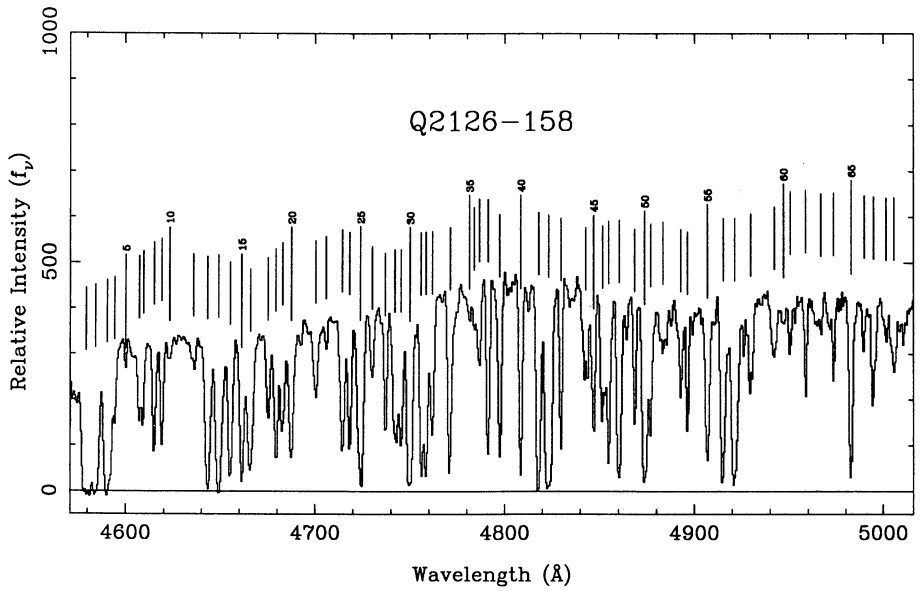

FIG. 3.—CCD spectrum with ~1 Å resolution of the region containing the Lyman-α line corresponding to the Lyman limit at $z_{abs} = 2.9676$

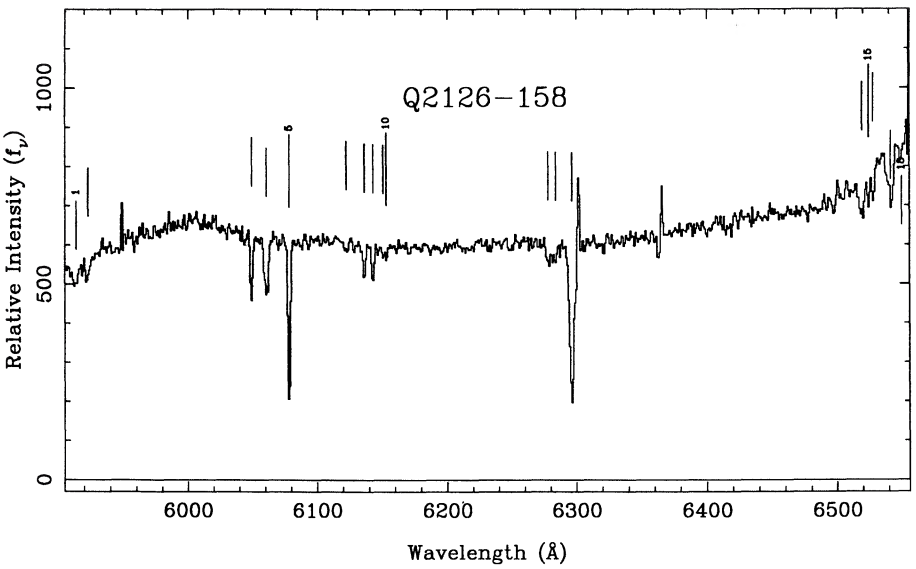

FIG. 4.—CCD spectrum with ~1.5 Å resolution of the region containing the putative C IV doublet corresponding to the Lyman limit at $z_{abs} = 2.9676$

Young *et al.* (1979) were confirmed, and two additional weak systems, $z_{abs} = 2.4597$ and $z_{abs} = 2.6791$, were found. No certain heavy element lines associated with the Lyman limit system at $z_{abs} = 2.97$ were found in these new spectra. Meyer and York (1987) found three additional weak systems in their study of a restricted wavelength range, namely, $z_{abs} = 2.7279$, 2.8194, and 2.9075.

The new line lists given in Tables 2–5 were analyzed using the methods outlined by Young *et al.* (1979). The resulting identifications are given in the last two columns of these tables. Nine absorption redshifts were found; the cases for five of these were given in § IIIyy of SBS.

$z_{abs} = 2.9676$.—The identification of three relatively strong lines with Lyα, Lyβ, and Lyγ puts the system beyond doubt. The higher Lyman series lines are in some cases blended with lines from other redshift systems; however the series is clearly observed to converge to the Lyman limit which is responsible for the pronounced break in the spectrum at 3650 Å (see Fig. 1). Some residual intensity is observed below 3640 Å and, from an inspection of Figure 1, it appears that the Lyman continuum in PKS 2126−158 is not completely opaque until ~3450 Å. It may immediately be deduced that the optical depth in the Lyman continuum in the $z_{abs} = 2.9676$ system is not large, but is of order unity. Accordingly, the column density for this system must be about $N(\text{H I}) \sim 10^{17}$ cm^{-2}. A more detailed analysis of the system will be given in § IV. As will be seen in § IV, the $z_{abs} = 2.9676$ system has an accompanying weaker system at $z_{abs} = 2.9635$.

$z_{abs} = 2.9076$.—A C IV doublet corresponding to this redshift was identified by Meyer and York (1987). We identify the corresponding Lyman-α line, together with several higher Lyman series members. We also identify C II λ977 and Si III λ1206 in the Lyman-α forest, together with Al II λ1670.

$z_{abs} = 2.8194$.—We found Lyman-α, Lyman-β, C III λ977, and Si III λ1206 corresponding to the C IV doublet found by Meyer and York.

$z_{abs} = 2.7685$.—This system is further strengthened by the discovery of additional lines in the new data. Lyman-β and Lyman-γ are seen as very strong lines at $\lambda\lambda$3865.47 and 3665.06, respectively. Several lines in the Lyman-α forest can be identified with heavy element lines in this system. These include λ3889.3 and λ3911.4, which could be identified with the O VI $\lambda\lambda$1031, 1037 doublet; however, the wavelength agreement is not good, and it is surprising that N V $\lambda\lambda$1238, 1242 are not observed. C II λ1036 and C III λ977 are possibly present. Longward of the Lyman-α forest, an otherwise unidentified line corresponds to Al II λ1670 in this system.

$z_{abs} = 2.7279$.—We find the Lyman-β line corresponding to the C IV doublet found by Meyer and York at this redshift. The Lyman-α line is listed in Table 3 of Young *et al.* (1979).

$z_{abs} = 2.6791$.—A weak C IV doublet at this redshift was found by SBS. We find Lyman-β; a strong line at λ4474.3, which could be Lyman-α, is given in Young *et al.* (1979).

$z_{abs} = 2.6379$.—A pair of strong lines at λ3754.4 and λ3774.5 could be the O VI $\lambda\lambda$1031, 1037 doublet in this system; however, λ3774.5 is already identified as Lyman-β at $z_{abs} = 2.6791$ and the N V doublet is not observed. Thus, as in the cases of $z_{abs} = 2.9676$ (see § IV) and $z_{abs} = 2.7685$, there is no strong evidence for the existence of O VI absorption. Lyman-β is added to the previously known lines in this system.

$z_{abs} = 2.4597$.—A weak C IV doublet at this redshift was identified by SBS. We add Lyman-α and Si II λ1260.

$z_{abs} = 2.3939$.—In the earlier work of Young *et al.* (1979), the provenance of this system relied mainly on the identification of the C IV doublet $\lambda\lambda$1548, 1550; however, λ1548 was blended with Si IV λ1393 in $z_{abs} = 2.7685$. The new data reveal three additional lines: S II $\lambda\lambda$1260, Si III λ1206, and Lyman-α λ1216. This system is now, therefore, beyond doubt.

Finally, we draw attention to a possible absorption system which does not satisfy the normal criteria for inclusion in Tables 2–5.

$z_{abs} = 2.0227$.—This system has the property that all of the identified lines are in the Lyman-α "forest"; consequently, the fact that it identifies 11 lines is not completely convincing in itself. On the other hand, all of the identified lines are strong, particularly Lyman-α with $W = 8.17$ Å. Moreover, the C IV $\lambda\lambda$1548, 1550 doublet ratio is reasonable, as are the relative strengths of the lines of other ions.

TABLE 2

ABSORPTION LINES IN THE SPECTRUM OF PKS 2126−158

No.	λ_{obs}	$\sigma(\lambda)$	W_{obs}	$\sigma(W)$	S/N	ID	z_{abs}
				3760–4415 Å			
1	3763.97	0.13	0.96	0.15	6.2	HI(949)	2.9631
2	3769.05	0.12	3.15	0.20	6.3	HI(949)	2.9685
3	3771.80	0.12	0.83	0.14	6.3		
4	3774.45	0.11	2.69	0.19	6.4	HI(1025)	2.6798
5	3777.33	0.13	1.02	0.15	6.3		
6	3780.13	0.11	2.71	0.19	6.4		
7	3782.85	0.12	1.17	0.14	6.8		
8	3797.21	0.13	1.60	0.17	6.8		
9	3800.33	0.12	1.42	0.15	6.9	HI(972)	2.9076
10	3805.34	0.12	0.87	0.13	7.0		
11	3807.04	0.11	0.98	0.12	7.0		
12	3809.80	0.15	1.42	0.18	7.0		
13	3813.55	0.14	1.91	0.18	7.2		
14	3817.80	0.12	3.40	0.20	7.2	CIII(977)	2.9076
15	3824.39	0.11	2.03	0.16	7.4	HI(1025)	2.7285
16	3826.94	0.12	1.07	0.13	7.3		
17	3835.24	0.12	0.67	0.11	8.1		
18	3841.51	0.13	0.75	0.12	8.4		
19	3845.20	0.11	1.24	0.11	8.8		
20	3847.11	0.12	1.02	0.11	8.6		
21	3854.95	0.12	1.34	0.13	9.1	HI(972)	2.9638
22	3859.05	0.10	2.68	0.13	9.5	HI(972)	2.9680
23	3866.21	0.12	7.71	0.22	9.5	HI(1025)	2.7693
24	3873.55	0.11	2.81	0.14	9.7		
25	3876.96	0.11	2.11	0.12	10.2	CIII(977)	2.9681
26	3889.28	0.11	2.15	0.12	10.7	OVI(1032)	2.7689
27	3892.44	0.12	1.33	0.11	10.5		
28	3895.23	0.11	0.94	0.09	10.7		
29	3898.46	0.11	2.66	0.13	10.5		
30	3902.29	0.11	1.74	0.11	10.4		
31	3905.79	0.11	2.19	0.13	10.3		
32	3911.39	0.15	1.58	0.14	10.2	OVI(1037)	2.7696
33	3918.37	0.12	3.66	0.16	10.1	HI(1025)	2.8201
34	3922.90	0.11	2.24	0.12	10.2		
35	3927.03	0.11	3.74	0.15	10.1		
36	3937.05	0.11	1.93	0.11	11.1		
37	3942.20	0.12	1.96	0.12	11.1		
38	3955.00	0.11	1.22	0.10	10.9		
39	3957.10	0.10	1.20	0.08	10.9		
40	3959.45	0.10	1.78	0.10	10.7		
41	3962.27	0.11	2.24	0.12	10.8		
42	3966.82	0.13	1.89	0.14	10.6		
43	3986.62	0.12	1.66	0.11	12.1		
44	3993.97	0.10	1.45	0.09	12.8		
45	3998.56	0.10	2.89	0.11	12.9		
46	4002.10	0.13	0.56	0.08	12.7		
47	4005.08	0.11	1.22	0.09	12.9		
48	4007.88	0.10	2.38	0.10	12.9	HI(1025)	2.9074
49	4011.96	0.10	3.24	0.11	12.6		
50	4015.86	0.10	3.52	0.12	12.4		
51	4025.46	0.13	0.80	0.09	12.2		
52	4033.48	0.11	1.67	0.11	12.2		
53	4042.49	0.14	0.52	0.08	12.8		
54	4048.76	0.16	0.56	0.09	12.6		
55	4053.57	0.13	1.14	0.10	12.7		
56	4057.47	0.11	1.15	0.09	13.0		
57	4065.48	0.10	1.92	0.09	13.2	HI(1025)	2.9635
58	4069.21	0.10	3.81	0.12	13.2	HI(1025)	2.9672
59	4075.88	0.14	1.05	0.10	13.2	HI(1025)	2.9737
60	4084.96	0.11	1.70	0.10	13.4		
61	4090.22	0.12	0.69	0.08	13.4		
62	4094.68	0.11	1.56	0.10	13.6	SiIII(1206)	2.3938
63	4101.21	0.10	1.94	0.09	14.2		
64	4113.30	0.11	2.22	0.10	14.0		
65	4116.74	0.14	0.63	0.08	14.1		
66	4120.12	0.13	1.09	0.10	14.0		
67	4126.07	0.11	4.64	0.13	13.8	HI(1215)	2.3941
68	4133.81	0.12	0.88	0.08	14.2		
69	4146.52	0.13	1.39	0.10	14.4		
70	4152.72	0.11	1.68	0.09	14.5		
71	4157.94	0.11	1.59	0.09	14.8		
72	4162.79	0.13	0.60	0.08	14.0		
73	4165.24	0.11	0.79	0.08	13.9		

TABLE 2.—*Continued*

No.	λ_{obs}	$\sigma(\lambda)$	W_{obs}	$\sigma(W)$	S/N	ID	z_{abs}
			3760–4415 Å				
74	4173.20	0.13	0.62	0.08	13.3	SiIII(1206)	2.4589
75	4176.97	0.11	3.64	0.12	13.4		
76	4185.49	0.11	1.56	0.10	13.0		
77	4198.56	0.12	2.83	0.13	12.7		
78	4205.69	0.10	3.76	0.13	12.7	HI(1215)	2.4596
79	4212.30	0.11	2.39	0.11	13.4		
80	4236.75	0.11	4.28	0.14	13.1		
81	4241.87	0.10	2.06	0.10	13.1		
82	4244.56	0.10	1.36	0.08	13.2		
83	4254.08	0.12	0.55	0.07	13.2		
84	4265.04	0.13	0.58	0.08	13.6		
85	4273.62	0.12	1.71	0.11	13.9	FeII(1133)	2.7697
86	4277.17	0.13	0.80	0.09	13.8	SiII(1260)	2.3935
87	4284.30	0.10	3.04	0.11	14.3		
88	4295.43	0.12	0.98	0.08	14.4		
89	4301.05	0.11	1.27	0.09	14.4		
90	4304.61	0.12	1.52	0.10	14.6		
91	4310.47	0.13	0.59	0.08	14.4		
92	4314.30	0.15	0.63	0.09	13.8		
93	4323.08	0.11	6.18	0.16	13.4		
94	4329.94	0.11	2.39	0.11	13.5		
95	4339.53	0.11	5.14	0.14	13.3		
96	4353.36	0.24	1.01	0.14	11.6		
97	4360.45	0.13	1.45	0.12	11.4	SiII(1260)	2.4595
98	4367.76	0.13	0.64	0.10	10.4		
99	4382.85	0.16	1.35	0.15	9.6		
100	4389.91	0.13	2.95	0.17	9.8	SiIII(1206)	2.6385
101	4398.92	0.12	1.03	0.12	9.5		
102	4402.60	0.12	1.05	0.12	9.4		
103	4409.68	0.12	0.82	0.11	8.9		

IV. THE LYMAN LIMIT SYSTEM $z_{abs} = 2.97$

We have seen that the Lyman edge visible in Figure 2 is produced by an absorption system at $z_{abs} = 2.97$. A closer examination of the spectra reveals that there are two strong sets of Lyman series lines with similar equivalent widths at $z_{abs} = 2.9635 \pm 0.0002$ and $z_{abs} = 2.9678 \pm 0.0003$. These systems are sufficiently close together that both contribute to the observed Lyman edge.

As may be seen in Figure 2, there is some radiation shortward of the Lyman edge, implying that the Lyman-continuum optical depth in this pair of systems is not large. After various trials at drawing in the continuum levels on either side of the discontinuity, attempting to take into account for example a possible depression in the continuum level due to overlapping absorption lines on the long-wavelength side, we estimate that the ratio of the continuum fluxes on the two sides of the Lyman limit is $I^-/I^+ = 0.20 \pm 0.07$. The quoted error expresses the range in values obtained in the different trials, and is thus not a statistical error. For comparison, the value obtained by Sargent, Steidel, and Boksenberg (1989) from the low-resolution slit spectrophotometry was $I^-/I^+ = 0.10$, in satisfactory agreement with our new value. The size of the Lyman jump is related to the H I column density by

$$I^-/I^+ = e^{-\tau_{LL}}, \quad (1)$$

where $\tau_{LL} = 6.3 \times 10^{-18} N(\text{H I})$. This leads to a very accurate estimate of the total column density for the two systems,

$$17.32 < \log N(\text{H I}) < 17.51 . \quad (2)$$

An interactive computer program which simultaneously fits Voigt profiles to the Lyman series lines and calculates the shape of the convergence of the Lyman series, all convolved with the instrumental profile, was used to obtain column densities (or limits) for the two absorption systems discussed above. The resulting column densities were

$$z_{abs} = 2.9635 : \quad \log N(\text{H I}) \leq 16.0 \text{ cm}^{-2} ,$$

$$z_{abs} = 2.9676 : \quad \log N(\text{H I}) = 17.35 \pm 0.1 \text{ cm}^{-2} ,$$

$$\sigma = 30 \pm 3 \text{ km s}^{-1} .$$

Thus the total column density contributing to the Lyman discontinuity is $\log N(\text{H I}) \approx 17.35$, in good agreement with that inferred from the Lyman discontinuity alone. Since the system with $z_{abs} = 2.9635$ makes a negligible contribution to the Lyman discontinuity, we will constrain most of the discussion to the system with $z_{abs} = 2.9676$ from now on.

The expected wavelengths of the C IV $\lambda\lambda$1548, 1550 doublet corresponding to the redshift of the Lyman discontinuity are 6142.63 and 6152.83 Å, respectively. As can be seen from Figure 4 and Table 5, weak C IV lines are observed at the expected positions. A normalized plot of this part of the spectrum, with the calculated line profiles superposed, is shown in Figure 5. We see that there are also features at the expected positions of the C IV $\lambda\lambda$1548, 1550 lines at $z_{abs} = 2.9635$, although the λ1550 line is too weak to appear in Table 5. In order to give the reader an impression of the likely reality of the C IV doublets identified in Figure 5, we show for comparison in Figure 6 a nearby region of the spectrum containing no measured features. As indicated in Table 5, both features attributable to C IV λ1548 may be blended with lines from

TABLE 3

ABSORPTION LINES IN THE SPECTRUM OF PKS 2126−158

No.	λ_{obs}	$\sigma(\lambda)$	W_{obs}	$\sigma(W)$	S/N	ID	z_{abs}
				3125–4175 Å			
1	3664.61	0.22	8.31	0.26	11.1	HI(972)	2.7681
						+HI(937)	2.9077
2	3674.11	0.22	8.16	0.29	10.3		
3	3682.27	0.23	5.17	0.26	9.6	CIII(977)	2.7689
4	3688.27	0.24	1.92	0.19	10.5		
5	3692.17	0.22	3.35	0.21	10.3		
6	3703.10	0.23	2.35	0.20	10.0		
7	3711.20	0.25	2.36	0.23	9.6	HI(949)	2.9076
8	3715.87	0.23	2.56	0.21	9.8		
9	3720.42	0.22	2.68	0.21	9.5	HI(937)	2.9672
10	3726.18	0.23	1.91	0.19	9.4		
11	3732.09	0.24	6.06	0.32	8.9	HI(1025)	2.6385
						+CIII(977)	2.8198
12	3740.26	0.24	2.25	0.22	9.3		
13	3745.95	0.29	1.27	0.21	9.7		
14	3754.40	0.27	2.45	0.25	9.7	OVI(1032)	2.6382
15	3769.36	0.23	3.95	0.23	10.4	HI(949)	2.9688
16	3774.45	0.23	2.84	0.22	10.3	OVI(1037)	2.6376
						+HI(1025)	2.6798
17	3780.60	0.23	4.20	0.24	10.7		
18	3796.44	0.23	1.47	0.16	11.2		
19	3799.88	0.22	1.93	0.16	11.4	HI(972)	2.9072
20	3806.30	0.23	1.36	0.16	11.7		
21	3809.70	0.24	1.33	0.16	11.4		
22	3816.98	0.23	3.94	0.23	11.5	CIII(977)	2.9067
23	3825.47	0.25	3.64	0.24	11.6		
24	3845.31	0.30	2.21	0.23	11.5		
25	3854.76	0.24	1.50	0.16	13.3	HI(972)	2.9636
26	3858.95	0.23	2.71	0.18	12.8	HI(972)	2.9679
27	3865.96	0.22	7.17	0.24	11.8	HI(1025)	2.7690
28	3874.33	0.24	4.56	0.23	12.9		
29	3889.14	0.24	2.64	0.20	11.5	OVI(1032)	2.7687
30	3896.71	0.23	2.95	0.21	11.1		
31	3901.12	0.22	1.95	0.17	11.3		
32	3905.25	0.23	2.22	0.17	12.5		
33	3911.07	0.29	1.07	0.17	12.8	OVI(1037)	2.7692
34	3918.02	0.23	3.28	0.20	12.3	HI(1025)	2.8198
35	3922.82	0.21	2.40	0.15	12.8		
36	3926.43	0.21	3.93	0.17	13.3		
37	3936.37	0.24	2.01	0.17	13.7		
38	3942.25	0.26	2.34	0.20	12.9		
39	3958.48	0.27	6.13	0.30	11.5		
40	3966.60	0.29	1.91	0.20	12.5		
41	3986.13	0.25	1.52	0.16	13.6		
42	3993.72	0.23	2.27	0.16	14.4		
43	3998.84	0.22	3.22	0.17	13.6		
44	4004.38	0.22	1.60	0.14	13.4		
45	4007.94	0.21	2.65	0.15	13.3	HI(1025)	2.9074
46	4013.54	0.23	7.25	0.25	13.1		
47	4033.26	0.31	1.41	0.19	12.3		
48	4057.12	0.28	1.17	0.16	13.7		
49	4065.33	0.24	2.40	0.18	13.6	HI(1025)	2.9634
50	4069.35	0.21	3.25	0.15	13.4	HI(1025)	2.9673
51	4084.65	0.30	2.34	0.23	12.3		
52	4094.56	0.25	1.77	0.18	12.4	SiIII(1206)	2.3937
53	4100.70	0.27	1.76	0.18	13.2		
54	4113.36	0.26	2.46	0.20	12.9		
55	4125.75	0.23	4.54	0.20	13.8	HI(1215)	2.3938
56	4146.49	0.31	1.02	0.17	13.5		
57	4152.44	0.25	1.62	0.17	13.6		
58	4157.58	0.26	1.42	0.16	14.1		

TABLE 4

ABSORPTION LINES IN THE SPECTRUM OF PKS 2126−158

No.	λ_{obs}	$\sigma(\lambda)$	W_{obs}	$\sigma(W)$	S/N	ID	z_{abs}
			4570–5016 Å				
1	4579.42	0.04	5.82	0.08	22.7		
2	4584.36	0.04	3.97	0.06	25.1		
3	4590.49	0.05	4.56	0.10	17.7		
4	4594.39	0.05	1.31	0.03	43.9		
5	4600.12	0.07	0.19	0.02	55.1	SiIII(1206)	2.8187
6	4607.26	0.04	1.19	0.03	44.4		
7	4609.42	0.04	0.82	0.03	44.2		
8	4615.04	0.04	1.57	0.03	49.7		
9	4619.07	0.04	1.36	0.03	45.4		
10	4623.16	0.07	0.27	0.02	55.7		
11	4635.79	0.08	0.50	0.03	56.4	SiII(1260)	2.6780
12	4643.25	0.04	3.43	0.04	43.9	HI(1215)	2.8195
13	4649.07	0.04	3.95	0.05	31.5		
14	4655.16	0.04	2.71	0.04	39.3		
15	4661.24	0.04	2.66	0.04	43.1		
16	4665.97	0.04	3.17	0.05	35.3		
17	4675.18	0.04	1.24	0.03	48.6		
18	4679.31	0.04	2.07	0.04	36.5		
19	4682.84	0.04	1.76	0.03	43.8		
20	4687.52	0.04	2.39	0.04	37.7		
21	4700.37	0.05	1.26	0.03	51.1		
22	4705.87	0.07	0.26	0.02	60.3		
23	4714.48	0.04	2.16	0.04	45.1	SiIII(1206)	2.9075
24	4718.35	0.04	1.76	0.03	55.6		
25	4723.96	0.04	3.47	0.05	33.5		
26	4730.13	0.05	0.80	0.02	63.4	SiIV(1393)	2.3938
27	4736.96	0.04	1.35	0.03	57.8	OI(1302)	2.6377
28	4742.03	0.04	2.23	0.03	47.7		
29	4745.26	0.04	1.98	0.03	41.0	SiII(1304)	2.6380
30	4750.02	0.04	3.72	0.04	42.9	HI(1215)	2.9073
						+SiII(1260)	2.7686
31	4755.81	0.04	1.91	0.03	48.3		
32	4758.33	0.04	2.16	0.06	19.1		
33	4761.79	0.04	1.63	0.03	44.9		
34	4771.22	0.04	2.46	0.04	48.6		
35	4781.26	0.05	0.35	0.02	69.0	SiIII(1206)	2.9629
36	4783.79	0.05	0.39	0.02	60.2		
37	4786.54	0.04	0.79	0.02	62.5	SiIII(1206)	2.9673
38	4791.15	0.04	1.64	0.03	56.4	OI(1302)	2.6794
39	4797.28	0.04	1.92	0.04	47.7		
40	4808.53	0.04	1.96	0.03	42.6		
41	4818.10	0.04	3.12	0.04	45.9	HI(1215)	2.9635
42	4823.35	0.04	4.52	0.05	37.2	HI(1215)	2.9676
43	4829.81	0.04	1.30	0.03	41.4	HI(1215)	2.9730
44	4842.79	0.04	1.40	0.03	54.4		
45	4846.97	0.04	1.51	0.03	47.9		
46	4851.74	0.04	1.66	0.03	52.6		
47	4854.92	0.04	1.95	0.03	49.3	CII(1334)	2.6379
48	4860.42	0.04	2.65	0.05	33.4		
49	4868.55	0.04	1.08	0.02	59.8		
50	4873.69	0.04	2.90	0.05	28.0		
51	4876.93	0.04	1.65	0.04	39.9		
52	4883.47	0.06	0.91	0.03	48.8		
53	4892.88	0.06	1.22	0.04	48.2		
54	4896.36	0.05	1.21	0.04	39.6		
55	4906.92	0.05	2.38	0.05	33.9	OI(1302)	2.7683
56	4915.18	0.04	2.87	0.05	34.1	SiII(1304)	2.7682
57	4921.27	0.05	3.69	0.08	22.8		
58	4929.69	0.06	1.41	0.04	42.8		
59	4942.05	0.06	0.99	0.04	48.1		
60	4946.94	0.08	0.35	0.03	53.6		
61	4950.52	0.07	0.60	0.03	49.3		
62	4958.56	0.05	0.81	0.03	46.0		
63	4966.61	0.06	0.31	0.02	49.3		
64	4973.39	0.06	0.70	0.03	46.0		
65	4982.79	0.05	2.29	0.04	43.4		
66	4989.80	0.10	0.48	0.03	50.8		
67	4994.79	0.05	1.32	0.04	43.5	SiII(1260)?	2.9628
68	5001.45	0.08	0.44	0.03	49.6	SiII(1260)	2.9681
69	5005.60	0.05	0.98	0.03	41.0		

TABLE 5

ABSORPTION LINES IN THE SPECTRUM OF PKS 2126−158

No.	λ_{obs}	$\sigma(\lambda)$	W_{obs}	$\sigma(W)$	S/N	ID	z_{abs}
				5901–6556 Å			
1	5913.68	0.24	0.40	0.05	42.7	CIV(1548)	2.8197
2	5922.73	0.21	0.36	0.05	43.2	CIV(1550)	2.8192
3	6049.36	0.11	0.61	0.05	41.2	CIV(1548)	2.9073
4	6060.79	0.11	0.93	0.05	44.9	FeII(1608)	2.7681
						+CIV(1550)	2.9082
5	6078.35	0.06	1.60	0.04	59.6	AlII(1670)	2.6380
6	6122.36	0.19	0.14	0.02	81.1		
7	6136.22	0.08	0.35	0.02	89.3	CIV(1548)	2.9635
						+SiII(1808)?	2.3939
						+NaI(5891)?	0.0415
8	6142.86	0.06	0.36	0.02	88.7	CIV(1548)	2.9677
						+FeII(1608)?	2.8191
						+NaI(5897)?	0.0416
9	6150.64	0.11	0.11	0.02	89.5		
10	6153.11	0.10	0.12	0.02	91.6	CIV(1550)	2.9678
11	6278.03	0.15	0.23	0.04	45.3		
12	6283.92	0.16	0.15	0.03	44.3		
13	6296.47	0.05	2.81	0.05	53.4	AlII(1670)	2.7686
14	6519.27	0.12	0.50	0.03	70.5		
15	6524.34	0.12	0.21	0.02	69.1		
16	6527.82	0.12	0.22	0.03	68.4	AlII(1670)	2.9070
17	6541.33	0.13	0.83	0.04	64.2		
18	6549.76	0.21	0.48	0.04	58.0		

other redshifts.[2] Given that both features identified as C IV λ1548 lines have corresponding Lyman series absorption lines, the balance of the evidence would suggest that the putative C IV λ1548 features are not Na I D lines. Moreover, as shown by the dotted lines in Figure 5, both λ1548 features, together with their corresponding λ1550 features, can be fitted with optically thin C IV doublets. The parameters resulting from the fits are given in Table 6.

In order to set limits on the heavy element abundance in the Lyman limit redshift system, it is necessary to obtain information about the column densities of other ions. Sargent *et al.* (1979) showed that the observed abundances of various ions in the strong heavy element absorption systems in QSOs such as PKS 2126−158 could be explained on the hypothesis that the lines originated in a tenuous gas ionized by the metagalactic QSO flux (which was shown to dominate the expected flux from stars in the outer halos of high-redshift galaxies). Chaffee *et al.* (1986) used the metagalactic ionizing spectrum later published by Bechtold *et al.* (1987) and calculated grids of photoionization models in which the total hydrogen density was varied in order to set limits on the metal abundance in a Lyman-α forest cloud with a column density log N(H I) = 16.5. These authors pointed out that C III λ977 is expected to be the strongest observable feature over a wide range of total hydrogen density. On the basis of similar model calculations, we have searched our spectra of PKS 2126−158 for Si III λ1206 and C II λ1334, in addition to C III λ977. Both C III λ977 and

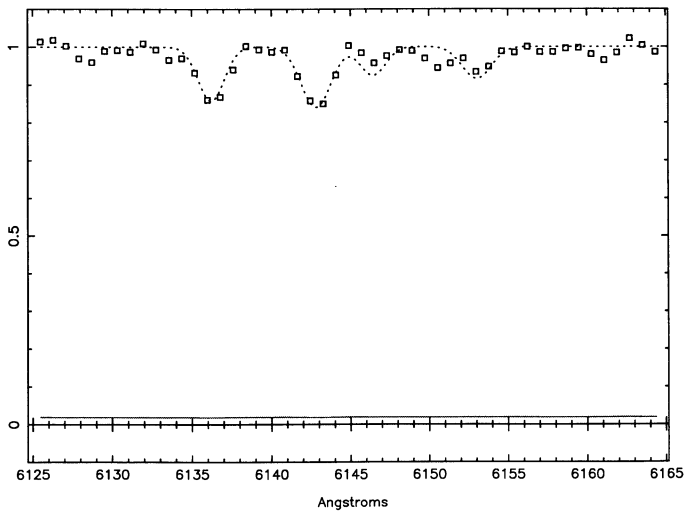

FIG. 5.—Normalized plot of the spectral region containing the two C IV doublets identified with the systems at $z_{abs} = 2.9635$ and $z_{abs} = 2.9676$. The points represent the actual data, while the dotted profiles are fits with the parameters given in Table 6. The hatched line at the bottom of the plot represents the 1 σ noise level for the data.

[2] The ratio of the wavelengths of the features attributed to C IV is $R = 1.00108 \pm 0.00002$, very close to the ratio of the rest wavelengths of the Na I D lines, $R_D = 1.00101$. We have seen that the λ1550 features are barely convincing, so that it is possible that the apparent C IV doublets associated with the Lyman limit at $z_{abs} = 2.9676$ are in fact due to Na I absorption at $z_{abs} = 0.04155$ (corresponding to a heliocentric recession velocity of 12,470 km s^{-1}). In this regard, it is interesting that deep CCD pictures taken with the Palomar 60 inch (1.5 m) telescope through Gunn g and r filters show two faint, extended objects located 5″ and 10″ west of the QSO (see Fig. 7). Both objects have $g \approx 20.8$ mag and $r \approx 20.5$ mag (the r calibration is rather uncertain), so that their absolute magnitudes would be $M_g \approx -16$ (using $H_0 = 50$ km s^{-1} Mpc^{-1}) if they are at a redshift of 12,470 km s^{-1}. A close inspection of the r frame indicates that the two objects are probably the brightest galaxies in a cluster; if this is the case, their redshift is much higher than 12,470 km s^{-1}. A more plausible value would be $z \approx 0.6$; we shall attempt to measure the precise value in the future. (At $z \sim 0.6$, the Ca II H and K lines would be redshifted to $\lambda_{obs} \sim 6300$. An inspection of Table 5 shows that none of the weak, unidentified absorption features can be identified with the Ca II doublet).

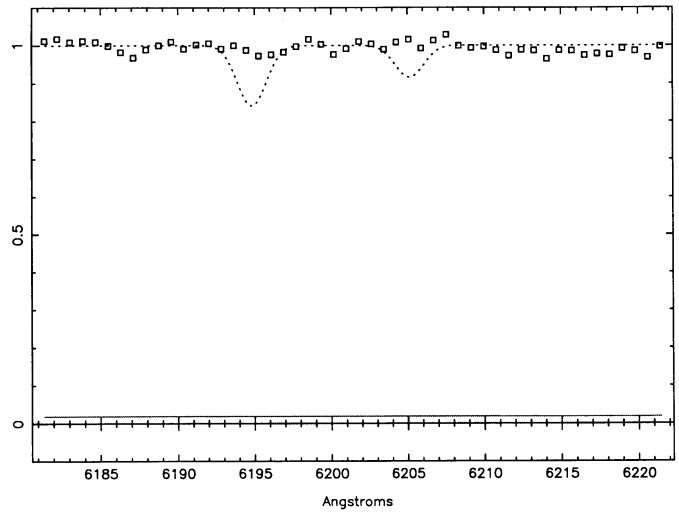

FIG. 6.—Normalized plot of a spectral region adjacent to that shown in Fig. 5. A C IV doublet profile with the strength of that identified with the $z_{abs} = 2.9676$ system is shown for comparison.

Si III λ1206 lie in the Lyman α forest;[3] consequently, the features observed at the appropriate wavelengths could largely be unassociated Lyman-α absorption lines. On the other hand, C II λ1334 falls in the continuum longward of the Lyman-α emission line in a region where no lines from other known absorption redshifts are expected. Measured column densities and column density limits for the two absorption systems are summarized in Table 6.

[3] An initial examination of the spectra indicated that the lines at 4094.65 Å and 4116.74 Å might be identifiable with the O VI $\lambda\lambda$1031, 1037 Å doublet. This possible identification is of particular interest because Norris, Hartwick, and Peterson (1983) and Peterson (1983) have claimed to have detected O VI in association with the Lyman-α forest lines in three other high-redshift QSOs by a statistical method in which the portions of spectra around the expected position of the O VI doublet were summed after being reduced to the rest frame determined by each Lyman-α line. In PKS 2126−158, λ4094.65 Å is already identified with Si III λ1206 in the certain system at $z_{abs} = 2.3938$. If the O VI identification is real this could explain why the observed doublet ratio is 2.56 as compared with the permitted upper limit of 2.0. On the other hand, 4116.74 Å is itself blended with the much stronger line 4113.27 Å and is not completely convincing as a separate feature. (Since we adopt the principle that lines must be found independently of their subsequent identification, we do not allow this post hoc judgment to change the line list.) Consequently, we do not regard the identification of the O VI doublet as being certain in the $z_{abs} = 2.9676$ system.

TABLE 6

COLUMN DENSITIES MEASURED FOR THE ABSORPTION SYSTEM AT $z_{abs} = 2.9676$

Ion	λ_0 (Å)	log N (cm^{-2})	σ (km s^{-1})	z_{abs}	Remarks
H I	Ly series	17.35 ± 0.1	30 ± 5	2.9676	
C II	1334.53	13.40 ± 0.1	(25)	2.9676	1
C III	977.03	≤ 14.3	(30)	(2.9676)	2
		≤ 14.8	(20)	(2.9676)	2
C IV	1548.20	13.40 ± 0.1	35	2.9676	3
Si II	1526.72	≤ 13.0	(30)	(2.9676)	2
Si III	1206.51	≤ 13.0	(30)	(2.9676)	1
Si IV	1393.72	≤ 12.8	(30)	(2.9676)	2

REMARKS.—(1) Probable detection, despite the fact that the line did not make the 5 σ cutoff for the line list. (2) Column density is an upper limit for the given velocity dispersion σ. (3) probable detection, although the lines may also be identified as lines from other systems (see text).

In determining actual abundances from the measurements of the ionic column densities, we have calculated models using the photoionization program CLOUDY, provided by Gary Ferland. While the actual dominant sources of ionizing radiation at high redshift are still uncertain, Steidel and Sargent (1989) have argued that the radiation field that ionizes the heavy element absorption systems, even at $z \approx 3$, cannot be dominated by hot stars in young galaxies, but rather it must have a spectral shape resembling those of AGNs. Thus, for the present purposes, the ionizing continuum is assumed to be in the shape of the "Medium" hardness integrated QSO spectrum calculated by Bechtold *et al.* (1987) (and thus the spectral shape of the ionizing radiation field is the same as that used by Chaffee *et al.* 1986; no particular strength of the ionizing continuum is assumed, but instead the models are calculated in terms of the ionization parameter

$$\Gamma = n_\gamma / n_H ,$$

where n_γ is the number density of photons capable of ionizing hydrogen incident on the face of the cloud, and n_H is the total number density of hydrogen. Thus, the models are similar to those of Bergeron and Stasinska (1986). Grids of models have been run in which the H I column density is fixed at the value determined from the observations and Γ is allowed to vary. The models then predict the relative column densities (for abundances scaled with solar values) for the various ionization stages of each element within the cloud; the value of Γ is then obtained by matching the observed relative column densities with the predicted ones. The measured column densities of C II, C III, and C IV are particularly useful for this determination, since essentially all of the carbon will be in one of these three ionization stages and lines of all three are often observed. When only upper limits can be placed on one or more of these column densities (as is sometimes the case, e.g., for the lines which fall in the Lyman-α forest, or when the heavy element abundances are low), then the ionization parameter can be constrained and in most cases an upper limit on the chemical abundance results. In these cases, the measured column densities (or limits) of Si II, Si III, Si IV, and in some instances a number of other ions, can be used as a test for consistency of the derived value of Γ. Details of the photoionization models and their use for the determination of chemical abundances and ionization states (including the uncertainties involved) in Lyman limit absorption systems will be discussed extensively in a forthcoming paper (Steidel 1990).

An example of the type of model grid used in determining Γ is shown in Figure 8. Once Γ has been determined based on the observational constraints available, the predicted ionization arrays for the various elements are used to transform ionic column densities into total column densities for each element. Using the methods described above, and assuming that the measured C II and C IV column densities are detections and not merely upper limits, we find that $\log \Gamma = -2.7 \pm 0.1$ for the system at $z_{abs} = 2.9676$ which gives rise to the Lyman discontinuity. The resulting carbon abundance in the cloud is

$$[C/H] = -2.3 \pm 0.2 ,$$

where the quoted errors reflect only the estimated uncertainty in the H I, C II, and C IV column densities (and the resulting uncertainty in Γ) and do not attempt to account for the uncertainties involved in applying the photoionization models to the problem in the first place. (Clearly the largest uncertainty lies in the ionization correction for hydrogen, since the models show

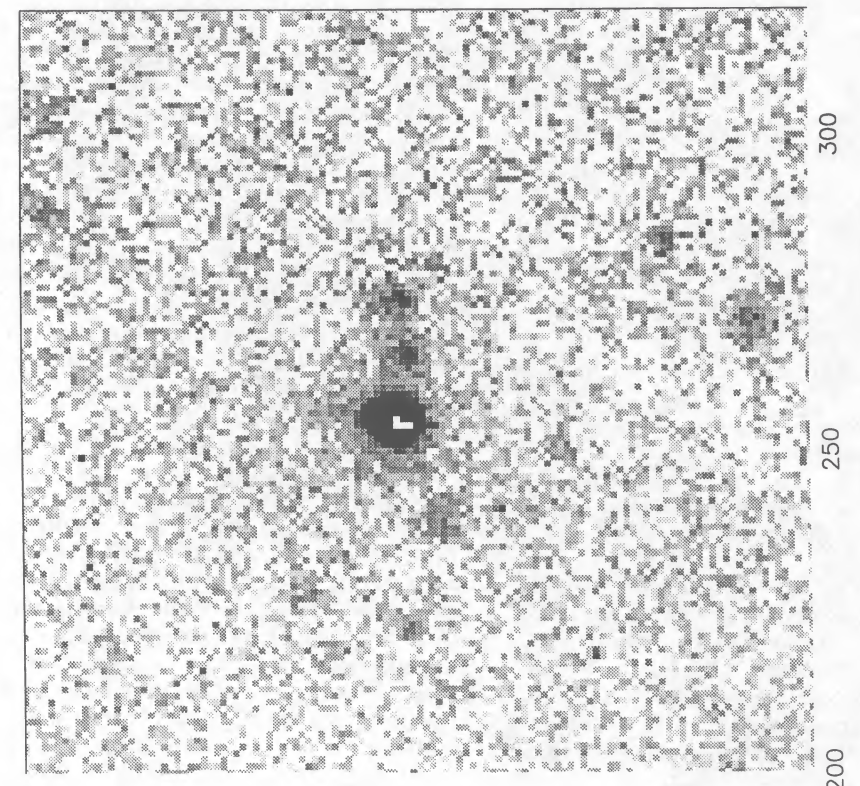

FIG. 7b

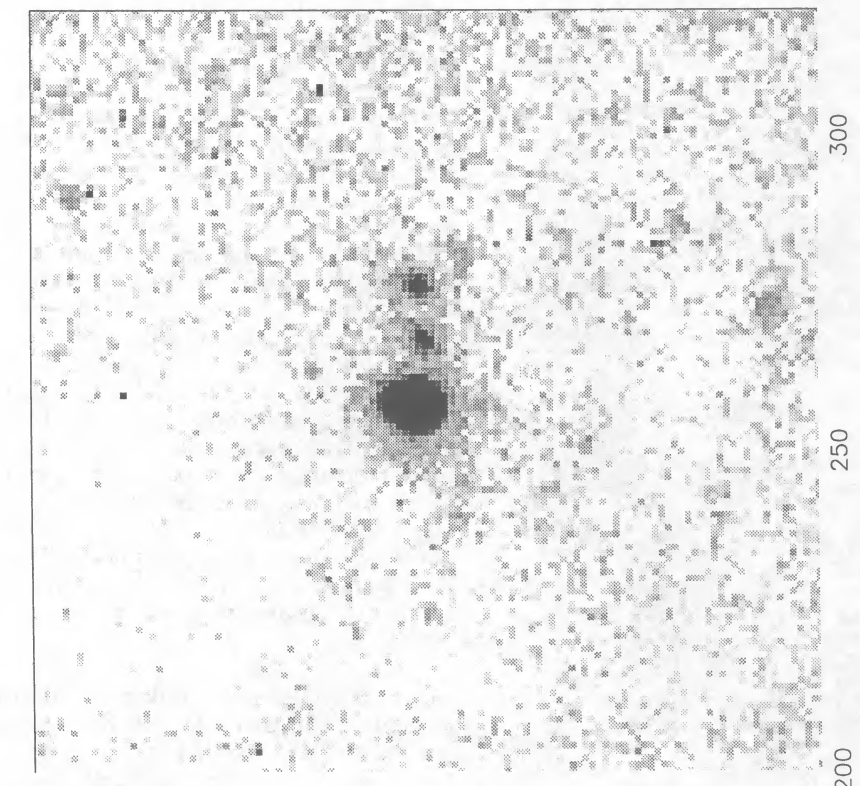

FIG. 7a

FIG. 7.—CCD pictures of the field containing PKS 2126−158 through (*a*) Gunn *g* filter, (*b*) Gunn *r* filter. The QSO is the bright object at the center of the field, while the two probable galaxies discussed in the text are directly to the west (right). The image scale is 0".47 pixel^{-1}.

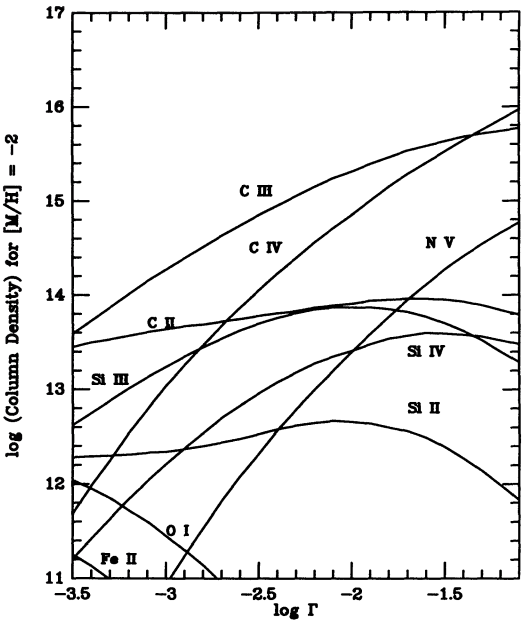

FIG. 8.—Photoionization model grid for a cloud having log N (H I) = 17.35. The ordinate shows the expected relative column densities for various ionic species, and the abscissa is the ionization parameter. The adopted value of Γ is based on the observations is log $\Gamma = -2.7 \pm 0.1$.

that typically the clouds are <1% neutral. However, experience has shown that consistent results can be obtained for the relative column densities of the heavy element species: Steidel 1989.) Using the model with log $\Gamma = -2.7$, the upper limits on the Si III and Si IV column densities (see Table 6) suggests that [Si/H] ≤ -2.3, consistent with a roughly uniform depletion of Si and C. It is interesting to note that, if the ionizing radiation field is assumed to be produced by hot stars (see Fig. 1*b* of Steidel and Sargent 1989), then log $\Gamma = -1.1$, and [C/H] ≈ -2.9; however, as pointed out by Steidel and Sargent (1989), the predicted column densities of Si III and Si IV are much too high, and an enormous total H column density is required, making this scenario unlikely.

We recall that the initial impetus to study the composition of the LLS in PKS 2126−158 stemmed from the possibility that it might be produced by a primordial H I cloud. We have now established that this cannot be correct; the value of [C/H], while low, is much higher than the limit of [C/H] ≤ -3.5 established by Chaffee *et al.* (1986) for a high H I column density cloud at $z_{abs} = 3.321$ in the Lyman-α forest observed in the spectrum of Q0014+813. It is still the case, however, that the discovery of LLSs in the spectra of high-redshift QSOs provides a promising avenue for detecting primordial H I clouds. Several candidates for such clouds were found in the Lyman limit survey of Sargent, Steidel, and Boksenberg (1989), and these are in the course of being studied by higher resolution observations.

V. CONCLUSIONS

In summary, the abundances in the $z_{abs} = 2.97$ Lyman limit system in PKS 2126−158 resemble those typically encountered in Galactic stars of Population II.[4] In such stars, [Fe/H], which is taken as a "benchmark" of the heavy element abundance, is typically a lower than [C/H] by ~0.2 dex (Tomkin, Sneden, and Lambert 1986). Thus, we might reasonably expect that [Fe/H] ~ −2.5 in the gas responsible for the Lyman limit system. This is comparable to the [Fe/H] value in the most metal-poor Galactic globular clusters, and well below the values encountered in the most extreme heavy element–poor local star-forming galaxies, such as I Zw 18 and Tol 65 ([Fe/H] ~ −2; Kunth and Sargent 1986). We note, however, that the average star fromation rate in these dwarf systems is inferred to be roughly constant with time, although it appears to occur in bursts separated by long quiescent periods. In consequence, the heavy element abundance is expected on the simple "closed box" model to increase linearly with time. Now, for $\Omega = 1$, epoch scales with redshift according to the relation $t = t_0(1 + z)^{-1.5}$, where t_0 is the present age of the universe. Thus, the heavy element abundance in dwarf galaxies like I Zw 18 at the epoch corresponding to $z \sim 3$ can be reasonably inferred to be a roughly a factor of 8 below the present value, namely [Fe/H] ~ −2.9. The heavy element composition of the LLS in PKS 2126−158 thus resembles both the extreme Population II abundances of stars created in the primitive Galactic halo, and the inferred early compositions of the extreme dwarf emission line galaxies. It would clearly be of interest to determine the heavy element compositions a sample of LLSs at much lower redshifts. If the absorption lines are primarily produced by primitive galactic halos, such as that in the Galaxy, then the distribution of composition is not expected to change radically with epoch. If, on the other hand, most of the absorption cross section is contributed by swarms of star-forming, gas-rich dwarf galaxies, as York *et al.* (1986) suggested for certain classes of QSO absorption systems, then the heavy element abundance might be expected to increase roughly linearly with time. It is hoped that future observations with the Hubble Space Telescope will settle this question.

We thank John Fordham and Keith Shortridge for help in setting up and running the IPCS detector used in the early observations. We also thank John Henning, Dave Tennant, Mike Doyle, and Skip Staples for their help at Palomar. The CLOUDY photoionization program was kindly provided by Gary Ferland. The work of A. B. was supported by the U.K. Science and Engineering Research Council. The beginning of the work was also supported by the National Science Foundation under grant AST 84-16704 to W. S.

[4] Based on a study in progress of a larger sample of LLSs, the heavy element abundance for this absorption system turns out to be typical of LLSs at $z \approx 3$ (Steidel 1990).

REFERENCES

Bergeron, J., and Stasinska, S. 1986, *Astr. Ap.*, **169**, 1.
Bechtold, J., Weymann, R. J., Lin, Z., and Malkan, M. A. 1987, *Ap. J.*, **315**, 180.
Chaffee, F. H., Foltz, C. B., Bechtold, J., and Weymann, R. J. 1986, *Ap. J.*, **301**, 116.
Jauncey, D. L., Wright, A. E., Peterson, B. A., and Condon, J. J. 1978, *Ap. J. (Letters)*, **223**, L1.
Kunth, D., and Sargent, W. L. W. 1986, *Ap. J.*, **300**, 496.
Meyer, D. M., and York, D. G. 1987, *Ap. J. (Letters)*, **315**, L5.
Norris, J., Hartwick, F. D. A., and Peterson, B. A. 1983, *Ap. J.*, **273**, 450.
Peterson, B. A. 1983, in *IAU Symposium 104, Early Evolution of the Universe and its Present Structure*, ed. G. Chincarini and G. O. Abell (Dordrecht: Reidel), p. 349.
Sargent, W. L. W., and Boksenberg, A. 1983, in *Quasars and Gravitational Lenses*. 24th Liège Astrophysical Colloquium, p. 518.
Sargent, W. L. W., Boksenberg, A., and Steidel, C. C. 1988, *Ap. J. Suppl.*, **68**, 539 (SBS).
Sargent, W. L. W., Steidel, C. C., and Boksenberg, A. 1989, *Ap. J. Suppl.*, **69**, 703.

Sargent, W. L. W., Young, P. J., Boksenberg, A., Carswell, R. F., and Whelan, J. A. J. 1979, *Ap. J.*, **230**, 49.
Steidel, C. C. 1990, in preparation.
Steidel, C. C., and Sargent, W. L. W. 1989, *Ap. J. (Letters)*, **343**, L33.
Tomkin, J., Sneden, C., and Lambert, D. L. 1986, *Ap. J.*, **302**, 415.
York, D. G., Dopita, M., Green, R., and Bechtold, J. 1986, *Ap. J.*, **311**, 610.
Young, P. J., Sargent, W. L. W., Boksenberg, A., Carswell, R. F., and Whelan, J. A. J. 1979, *Ap. J.*, **229**, 891.

A. BOKSENBERG: Royal Greenwich Observatory, Herstmonceux Castle, Hailsham, East Sussex BN27 1RP, England

W. L. W. SARGENT and C. C. STEIDEL: Palomar Observatory, 105-24, California Institute of Technology, Pasadena, CA 91125